International Journal of Engineering and Management Research
e-ISSN: 2250-0758 | p-ISSN: 2394-6962
Volume-11, Issue-1 (February 2021)
www.ijemr.net
https://doi.org/10.31033/ijemr.11.1.23

Landslide Susceptibility Assessment Using Modified Frequency Ratio Model in Kaski District, Nepal

Niraj Baral[1], Akhilesh Kumar Karna[2] and Suraj Gautam[3]

[1]Student, Department of Civil Engineering, Institute of Engineering, Pulchowk Campus / Tribhuvan University, NEPAL
[2]Visiting Faculty, Department of Civil Engineering, Institute of Engineering, Pulchowk Campus / Tribhuvan University, NEPAL
[3]Researcher, Natural Hazards Section, Institute of Himalayan Risk Reduction, NEPAL

[1]Corresponding Author: neerajbarals@gmail.com

ABSTRACT

Landslides are the most common natural hazards in Nepal especially in the mountainous terrain. The existing topographical scenario, complex geological settings followed by the heavy rainfall in monsoon has contributed to a large number of landslide events in the Kaski district. In this study, landslide susceptibility was modeled with the consideration of twelve conditioning factors to landslides like slope, aspect, elevation, Curvature, geology, land-use, soil type, precipitation, road proximity, drainage proximity, and thrust proximity. A Google-earth-based landslide inventory map of 637 landslide locations was prepared using data from Disinventar, reports, and satellite image interpretation and was randomly subdivided into a training set (70%) with 446 Points and a test set with 191 points (30%). The relationship among the landslides and the conditioning factors were statistically evaluated through the use of Modified Frequency ratio analysis. The results from the analysis gave the highest Prediction rate (PR) of 6.77 for elevation followed by PR of 6.45 for geology and PR of 6.38 for the landcover. The analysis was then validated by calculating the Area Under a Curve (AUC) and the prediction rate was found to be 68.87%. The developed landslide susceptibility map is helpful for the locals and authorities in planning and applying different intervention measures in the Kaski District.

***Keywords*—** Frequency Ratio, Kaski, Landslides, Susceptibility

I. INTRODUCTION

Among the natural hazards that occur frequently in Nepal, landslides are amongst the most serious one. Nepal is a landlocked country characterized by the high relief, rugged topography, complex geological conditions with active tectonic process and continued seismic activities. Around 83% of the total area of the country is occupied by the mountains and hills. Over the horizontal extent of around 90-120 km, the elevation of the country ranges from 60m (Terai) in the south to 8848m (Mount Everest) in the north. Because of the existing topographical variation and geological setting with heavy rainfall in monsoon season, the country frequently experiences landslides, debris flows, floods, and avalanches. These phenomena result in the loss of number of lives and huge amount of properties [1].

Landslide susceptibility is the assessment of the likelihood of a landslide in a specific area and it thus predicts where it is likely to occur [2]. There are number of methods and techniques that can be applied to develop landslide susceptibility maps in a study area [3]–[6]. The overall assessment of the susceptibility can be either qualitative or quantitative, and direct or indirect [7], [8]. Heuristic approach takes the expert judgements into account and thus is used as a tool for decision support system for the spatial decision. The subjective approaches through heuristic judgements are termed as qualitative method while quantitative method looks after the probabilities of occurrences of landslide phenomenon[7]. The quality of heuristic assessment largely depends on the capability of the experts to understand the ground reality and appropriate factors causing landslide in the area[9]. However, Quantitative method looks after the numerical assessment of the relationship between the controlling factors and can be either deterministic or statistical [5], [10], [11]. Thus, in this study, modified Frequency ratio (FR) method is used to derive the spatial relationship between the controlling factors with reference to the modified factor as used by different researchers [12]–[14]. Frequency ratio is a data driven quantitative method capable of performing Bivariate Statistical Analysis [15].

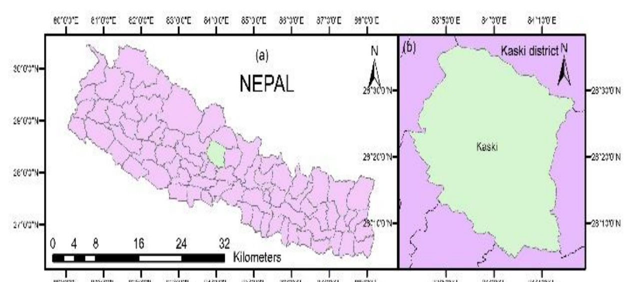

Figure 1: Location Map of Study Area

e-ISSN: 2250-0758 | p-ISSN: 2394-6962
Volume-11, Issue-1 (February 2021)
https://doi.org/10.31033/ijemr.11.1.23

The susceptibility map is prepared for the entire Kaski District. Kaski district is a part of the Gandaki Province with an area of 2017 sq. km. and total population of 492098 according to the 2011 Census. Kaski lies at the centroid part of the country with the altitude ranging from 450 metres to 8091 metres. The district is known for the Himalayan range with about 11 Himalayas with height greater than 7000 m. Besides, this district is also well known for the scenery of the northern mountains, gorge of Seti River, Davis Falls, natural caves, lakes and so on. Hence, it is one of the most famous tourist destinations in the world. More than 147 number of landslide events have been reported with around 288 death tolls in the Kaski district only for the last 50 years (1971- 2020)[16], [17]. Taking the average from the last 50 years, suggests that there are more than 5-6 fatalities recorded every year from the Kaski District only.

II. DATA

The datasets used in the generation of the susceptibility map is given in the Table 1. Twelve factors like Slope, aspect, elevation, curvature, geology, landcover, rock type, soil type, distance to drainage network, proximity to road, distance to lineament and precipitation are considered in the study as the conditioning factors.

Table 1: Datasets used in the study

Classification	**Map**	**GIS Data Type**	**Source**
Landslide Inventory	Landslide Inventory Map	Vector (Polygon)	Google Earth Imagery, Field Visit and Historical records
DEM	Slope Map	Raster Grid (12.5 x 12.5)	Derived from ALOS Palsar, Downloaded from USGS
	Aspect Map		
	Curvature Map		
	Elevation Map		
Geological Map	Lithology Map	Vector (shapefile)	Digitization of data from Geological Map of 1,000,000 scale published by Department of Mines and Geology in 1994.
Road Network	Proximity to road	Vector (shapefile)	Data compiled from Survey Department, Nepal. (Topographic map scale: 1:25,000 scale at Terai and Mid-Hills, and 1:50,000 scale at Upper Mountains and Himalayan range) https://data.humdata.org/dataset/ (Updated on 24 November 2015)
Hydrology	Distance to drainage network		
Soil and Terrain Database	Soil Type Map	Vector (shapefile)	Dijkshoorn JA and Huting JRM 2009. Soil and terrain database for Nepal (1:1 million)Report 2009/01 (available through: http://www.isric.org), ISRIC – World Soil Information, Wageningen (29 p. with data set)
Landcover Map	Land Cover Map	Raster (grid)	ICIMOD. (2013). Land cover of Nepal 2010 [Data set]. ICIMOD.
Precipitation	Precipitation Map	Vector(Point)	Department of Hydrology and Meteorology Nepal

III. METHODOLOGY

Using the Google Earth Images, the landslides were digitized and was then randomly divided into 70% training and 30% testing datasets. The datasets were then

e-ISSN: 2250-0758 | p-ISSN: 2394-6962
Volume-11, Issue-1 (February 2021)
https://doi.org/10.31033/ijemr.11.1.23

imported in the GIS environment and analyzed with the reclassified layers. The overall process of the study is given in the Fig 2.

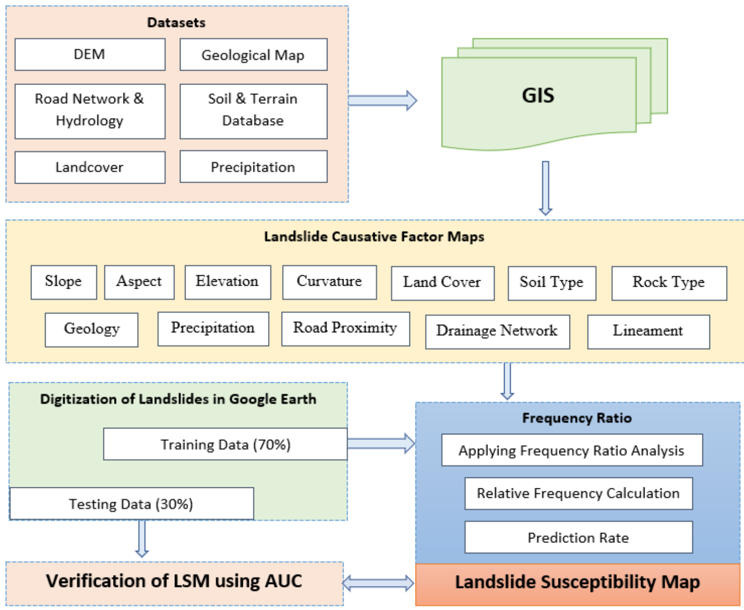

Figure 2: Work flow of the study

Figure 3: Landslide Causative Factor Maps in Kaski District

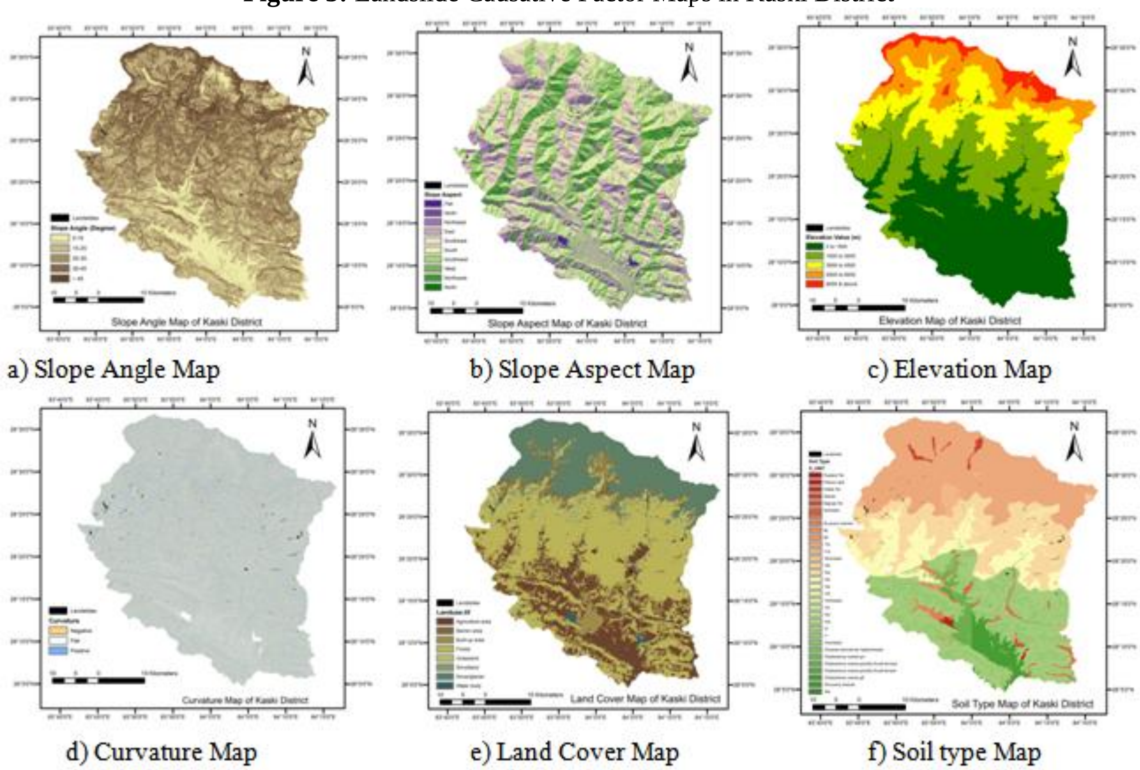

e-ISSN: 2250-0758 | p-ISSN: 2394-6962
Volume-11, Issue-1 (February 2021)
https://doi.org/10.31033/ijemr.11.1.23

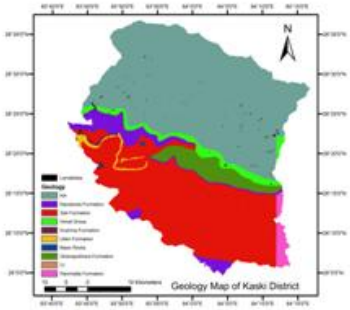

g) Geology Map

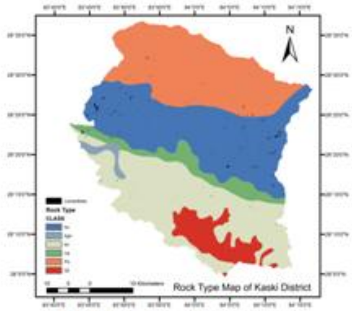

h) Rock type Map

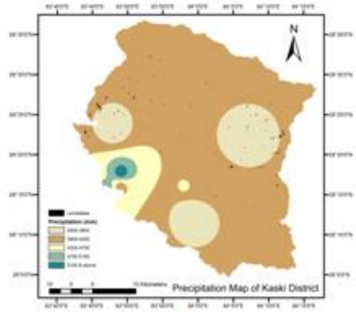

i) Precipitation Map

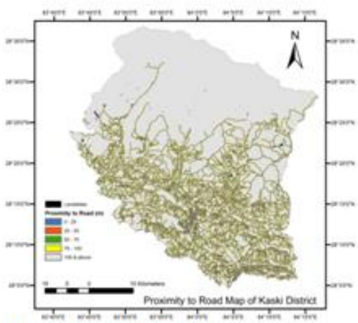

j) Road Proximity Map

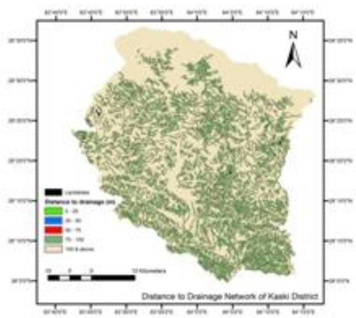

k) Drainage Network Map

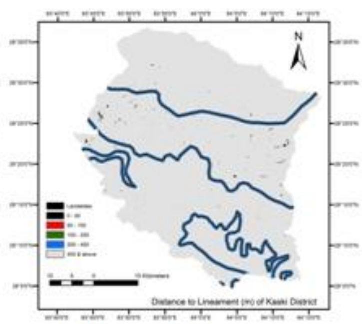

l) Lineament Map

Table 2: FR, RF and PR for each classes of the conditioning factors

Class	% Class Pixels	% Landslide Pixels	FR	RF	MIN RF(a)	MAX RF(b)	a-b (c)	MIN (a-b) (d)	PR (c/d)
Slope (Degrees)									
0-15	17.59%	4.36%	0.25	0.05	0.05	0.33	0.28	0.07	4.29
15-25	24.67%	14.80%	0.60	0.11					
25-35	27.86%	29.34%	1.05	0.20					
35-45	17.29%	29.57%	1.71	0.32					
45 & above	12.58%	21.93%	1.74	0.33					
Total	100.00%	100.00%	5.35						
Aspect									
Flat	0.72%	0.00%	0.00	0.00	0.00	0.32	0.32	0.07	4.89
N	4.60%	0.96%	0.21	0.03					
NE	9.32%	3.06%	0.33	0.05					
E	11.18%	10.10%	0.90	0.13					
SE	16.30%	36.20%	2.22	0.32					
S	17.06%	31.99%	1.88	0.27					
SW	15.59%	10.59%	0.68	0.10					
W	10.90%	3.94%	0.36	0.05					
NW	10.11%	2.53%	0.25	0.04					

e-ISSN: 2250-0758 | p-ISSN: 2394-6962
Volume-11, Issue-1 (February 2021)
https://doi.org/10.31033/ijemr.11.1.23

N	4.22%	0.63%	0.15	0.02					
Total	100.00%	100.00%	6.98						
Elevation									
0-1500	37.06%	19.20%	0.52	0.13	0.00	0.44	0.44	0.07	6.77
1500-3000	28.10%	49.52%	1.76	0.44					
3000-4500	18.27%	30.92%	1.69	0.42					
4500-6000	12.66%	0.37%	0.03	0.01					
6000 & above	3.91%	0.00%	0.00	0.00					
Total	100.00%	100.00%	4.00						
Geology									
No Data	48.96%	54.03%	1.10	0.09	0.00	0.42	0.42	0.07	6.45
Naudanda	5.16%	7.82%	1.52	0.13					
Seti	34.65%	16.99%	0.49	0.04					
Himal Group	3.54%	17.59%	4.97	0.42					
Kushma	0.35%	0.29%	0.81	0.07					
Ulleri	0.86%	2.23%	2.59	0.22					
Basic rocks	0.06%	0.00%	0.00	0.00					
Ghanapokhara	4.89%	0.70%	0.14	0.01					
Cr	0.00%	0.00%	0.00	0.00					
Ranimatta	1.52%	0.35%	0.23	0.02					
Total	100.00%	100.00%	11.85						

Class	**% Class Pixels**	**% Landslide Pixels**	**FR**	**RF**	**MIN RF(a)**	**MAX RF(b)**	**a-b (c)**	**MIN (a-b) (d)**	**PR (c/d)**
Land Cover									
Forest	44.39%	29.22%	0.66	0.05	0.00	0.42	0.42	0.07	6.38
Shrubland	2.37%	7.45%	3.14	0.24					
Grassland	5.82%	31.72%	5.45	0.42					
Agriculture	20.41%	21.83%	1.07	0.08					
Barren Area	4.56%	6.22%	1.36	0.10					
Water Body	1.05%	1.41%	1.34	0.10					
Snow/Glacier	20.06%	2.15%	0.11	0.01					
Built Up Atea	1.33%	0.00%	0.00	0.00					
Total	100.00%	100.00%	13.14						
Soil Type									
Rupakot Tal	0.06%	0.00%	0.00	0.00					
Phewa Lake	0.19%	0.00%	0.00	0.00					
Khalte Tal	0.00%	0.00%	0.00	0.00					

e-ISSN: 2250-0758 | p-ISSN: 2394-6962
Volume-11, Issue-1 (February 2021)
https://doi.org/10.31033/ijemr.11.1.23

Glacier	0.59%	0.19%	0.33	0.03					
Begnas Tal	0.11%	0.00%	0.00	0.00					
9c'	0.85%	0.22%	0.25	0.02					
9c	0.27%	0.00%	0.00	0.00					
9b pd	0.40%	0.00%	0.00	0.00					
9b	0.65%	0.00%	0.00	0.00					
9a	0.29%	0.00%	0.00	0.00					
17b	29.16%	17.20%	0.59	0.04					
17a	1.17%	1.48%	1.26	0.10					
16c'	0.12%	0.00%	0.00	0.00					
15b	17.82%	48.39%	2.72	0.21					
15a	1.79%	4.36%	2.44	0.18					
14b	8.10%	7.07%	0.87	0.07					
14a	2.82%	4.13%	1.46	0.11	0.00	0.21	0.21	0.07	3.17
13d	0.16%	0.17%	1.07	0.08					
13c'	0.07%	0.05%	0.76	0.06					
13c	0.02%	0.00%	0.00	0.00					
13b	0.02%	0.00%	0.00	0.00					
13a	0.06%	0.00%	0.00	0.00					
12	17.62%	8.93%	0.51	0.04					
11	11.26%	7.49%	0.67	0.05					
10c'	0.41%	0.07%	0.18	0.01					
10 ccth	0.25%	0.00%	0.00	0.00					
10 cc gvt	0.01%	0.00%	0.00	0.00					
10 cacgft	2.00%	0.01%	0.00	0.00					
10 ccgft	0.21%	0.00%	0.00	0.00					
10 ccg	3.42%	0.23%	0.07	0.01					
10b pd	0.09%	0.00%	0.00	0.00					
10a	0.00%	0.00%	0.00	0.00					
Total	100.00%	100.00%	13.19						

Class	**% Class Pixels**	**% Landslide Pixels**	**FR**	**RF**	**MIN RF(a)**	**MAX RF(b)**	**a-b (c)**	**MIN (a-b) (d)**	**PR (c/d)**
Rock Type									
hx	31.45%	67.13%	2.13	0.37					
Pz	27.56%	10.52%	0.38	0.07					
na	5.85%	7.76%	1.33	0.23					
kn	27.36%	12.61%	0.46	0.08	0.01	0.37	0.36	0.07	5.57
kgn	1.17%	1.61%	1.38	0.24					

e-ISSN: 2250-0758 | p-ISSN: 2394-6962
Volume-11, Issue-1 (February 2021)
https://doi.org/10.31033/ijemr.11.1.23

Ql	6.61%	0.37%	0.06	0.01					
Total	100.00%	100.00%	5.74						
Precipitation									
3500-3900	16.12%	30.09%	1.87	0.42	0.08	0.42	0.34	0.07	5.23
3900-4300	76.00%	65.24%	0.86	0.19					
4300-4700	6.17%	3.39%	0.55	0.12					
4700-5100	1.41%	1.17%	0.83	0.19					
5100 & above	0.30%	0.10%	0.35	0.08					
Total	100.00%	100.00%	4.46						
Road Proximity									
0-25	10.32%	6.16%	0.60	0.14	0.14	0.27	0.12	0.07	1.88
25-50	7.16%	5.29%	0.74	0.18					
50-75	6.52%	5.34%	0.82	0.20					
75-100	5.19%	4.73%	0.91	0.22					
>100	70.81%	78.48%	1.11	0.27					
Total	100.00%	100.00%	4.17						
Drainage Network									
0-25	12.88%	14.67%	1.14	0.21	0.16	0.23	0.07	0.07	1.00
25-50	9.90%	10.80%	1.09	0.20					
50-75	9.65%	11.04%	1.14	0.21					
75-100	7.99%	10.04%	1.26	0.23					
100-200	59.58%	53.45%	0.90	0.16					
Total	100.00%	100.00%	5.53						
Distance to Lineament									
0-50	1.34%	1.86%	1.39	0.29	0.09	0.29	0.19	0.07	2.99
50-100	1.22%	1.40%	1.14	0.24					
100-200	2.43%	1.92%	0.79	0.16					
200-400	4.83%	2.19%	0.45	0.09					
400 & above	90.18%	92.63%	1.03	0.21					
Total	100.00%	100.00%	4.80						
Curvature									
Negative	41.95%	45.26%	1.08	0.37	0.28	0.37	0.09	0.07	1.40
Flat	16.14%	13.18%	0.82	0.28					
Positive	41.91%	41.55%	0.99	0.34					
Total	100.00%	100.00%	2.89						

The spatial distribution and the extents of landslides are controlled by the different conditioning factors. Twelve factors are considered in our study and the subsequent thematic maps were generated in the GIS environment as shown in the Figure 3 (a to l). The Raster Grid (12.5 x 12.5) was considered and each conditioning factor were re-classified based on the different classes and properties. Individual area of each class for every factor was computed and the % of each class was determined.

It is essential to understand the physical conditions, context specific and morphology for triggering the landslides. Frequency ratio is one of the widely used

e-ISSN: 2250-0758 | p-ISSN: 2394-6962
Volume-11, Issue-1 (February 2021)
https://doi.org/10.31033/ijemr.11.1.23

quantitative technique for landslide susceptibility assessment using GIS techniques and spatial data.[11], [23]. Frequency ratio is mostly focused on the on the quantified assemblage between the landslide causative factors and the landslide inventories[24], [25]. Thus, Frequency ratio is computed as the ratio of landslide occurrence in a class to the total area of that class for the conditioning factor which is given as[26]

$$\mathbf{FR} = \frac{Npix(1)/Npix(2)}{\sum Npix(3)/\sum Npix(4)} \text{ ……………..(Eq. 1)}$$

where, $N_{pix(1)}$ = The number of pixels containing landslide in a class, $N_{pix(2)}$ = Total number of pixels of each class in the whole area, $\sum N_{pix(3)}$ = Total number of pixels containing landslide& $\sum N_{pix(4)}$ = Total number of pixels in the study area.

In order to ascertain the relative importance of each spatial factor with the available training dataset, the prediction rate (PR) was determined depending upon its degree of spatial association with the training landslide datasets[27].

$$\mathbf{PR} = \frac{RF_{max}-RF_{min}}{(RF_{max}-RF_{max})_{min}} \text{ ……………..(Eq. 2)}$$

Where, RF_{max}& RF_{min} is the maximum Relative Frequency among the classes within a factor while, $(RF_{max} - RF_{min})_{min}$ is the minimum value among all the factors considered. The subsequent value of each class for every conditioning factor in our study is shown in Table 2.

Finally, the Landslide Susceptibility Index (LSI) is obtained by combining PR and RF as:

$$\mathbf{LSI} = \sum_i PR_i \ x \ FR_i \text{ …... (Eq. 3)}$$

Where, $FR_i$is the rating of each factor's type and PR_i is the multiplier for each factor.

IV. RESULTS AND DISCUSSION

Using (Eq. 1), Frequency ratio for each class of a factor is calculated followed by the calculation of Prediction Ratio. Higher value of FR means the stronger association of the landslides and the conditioning factor.

Slope is one of the most important factor in the susceptibility mapping[18]–[20].Due to the influence of several conditions like geology, hydrology, morphological conditions, land use and so on, the landslides are observed on the different slopes[21].Slope ranging from 45^0& above, 35^0 to 45^0 have FR of 1.74 and 1.71 respectively. Hence, the greater number of landslides seems to be concentrated in the areas of those slopes. Besides, the number of landslide events are also determined by different parameters like sunlight, rainfall, drying winds and discontinuities [22].Thus, the slope aspect was derived from DEM and reclassified into nine classes: Flat (−1), North (0^0 - 22.5^0, 337.5^0-360^0), Northeast (22.5^0-67.5^0), East (67.5^0-112.5^0), Southeast (112.5^0-157.5^0), South (157.5^0-202.5^0), Southwest (202.5^0-247.5^0), West (247.50-292.50) and Northwest (292.5^0-337.5^0). The FR was found larger at the Slope aspects of South-East (2.22) and South (1.88) as compared to the others, thus signifying the higher probability of landslides in those facing slopes. Similarly, the landslides were found abundantly in the range of 3000-4500metres, 1500-3000 metres with FR 1.76 and 1.69 respectively. In our study, the distribution of the landslides is seen to be decreasing with the increase in elevation and there are negligible landslides with the elevation above 4500m. It also signifies that the there is no direct correlation between the higher elevation and landslides. Similarly, the negative curvature with FR 1.08 was found to have higher probability of landslide occurrences.

In case of geology, landslides were found abundant in the Himal Group and Ulleri Formation with the FR 4.97 and 2.59 respectively. Besides, Naudanda Formation and Kushma Formation also showed good relation to the landslide occurrence with FR 1.52 and 0.8 respectively. The factor landuse controls the slope stability as variability in vegetation cover influences the susceptibility of a slope to fail. The land use classes like Grassland and Shrubland with FR 5.45 and 3.14 respectively had the higher probabilities of landslide occurrences. The soil type of 15b and 15a (Past glaciated Mountainous Terrain above upper altitudinal limit of arable agriculture) with FR 2.72 and 2.44 showed the stronger relation to landslide occurrence. Similarly, the rock type with group Higher Himalayan Crystalline had the higher probability of landslides with FR 2.13.

Rainfall is one of the important parameters that affect the ground motion as it increases the pore pressure and increases soil moisture conditions on slope causing the issues on stability. Thus, the effect of precipitation is aggravated by the slope gradient and land cover[28]. The annual rainfall of 3500-3900m showed the higher FR value of 1.86. Besides, the existing road and the on-going constructions also disturbs the stability of slope thereby increasing the probability of landslide occurrence. The proximity of road above 100 metres had the highest FR value of 1.1 followed by proximity of road between 75-100 and 50-75 metres with FR values 0.82 and 0.74 respectively.

Similarly, water courses or drainage accumulate waters and saturate the surrounding surface and subsurface areas, rivers and drainage network plays a vital role in landslide occurrences[29], [30].The landslide occurrence probability was highest for the drainage buffer of 75-100mrange with FR 1.26 and also for the thrust proximity of 0 to 50m range with FR 1.39.

Using the value of FR, the Relative Frequency is calculated for all following factors. After the computation

e-ISSN: 2250-0758 | p-ISSN: 2394-6962
Volume-11, Issue-1 (February 2021)
https://doi.org/10.31033/ijemr.11.1.23

of RF, PR value for each factor was calculated using Eq.2 which is shown inFigure 4.

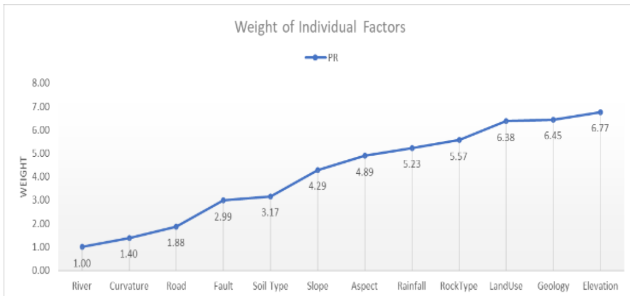

Figure 4: PR Value for each factor

Landslide susceptibility map(LSM) was then prepared by multiplying PR and FR for individual factor using the Eq. 3. The equation used for the preparation of LSM is given as:

LSM = *(1 x Distance to Drainage Network) + (1.4 x Curvature) + (1.88 x Proximity to Road) + (2.99 x Distance to Lineament) + (3.17 x Soil Type) + (4.29 x Slope Angle) + (4.89 x Slope Aspect) + (5.23 x Precipitation) + (5.57 x Rock Type) + (6.38 x Land Cover) + (6.45 x Geology) + (6.77 x Elevation) …….Eq (4)*

Using Eq 4 in the raster calculator of GIS environment, the susceptibility map was generated as shown in Figure 5.Thus, developed susceptibility map was then reclassified into five classes, i.e., very low, low, moderate, high and very high susceptibility classes. It indicated that 12.19% of the area has very high, 19.9% of the area has high while 15.93% has moderate, 23.12% has low and 28.86% has very low susceptibility to landslides.

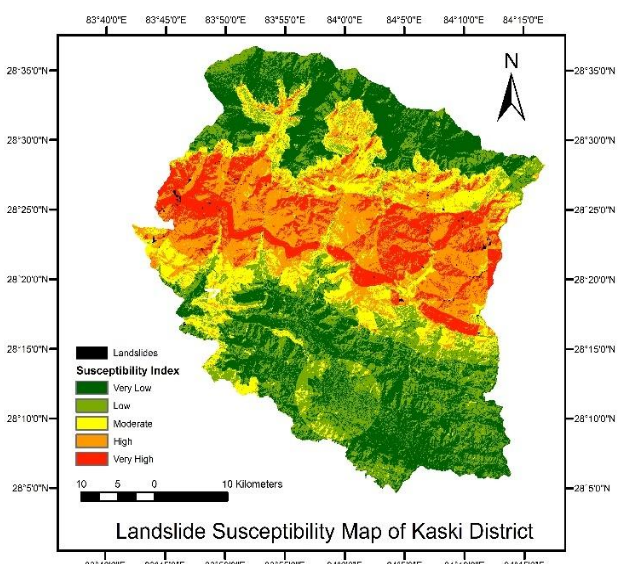

Figure 5: Landslide Susceptibility Map of Kaski

Validation

The produced landslide susceptibility map was then validated by using the training data used during the preparation of model with the susceptibility map. It was carried out to ascertain the predictability of the model and also look for the fitness of the model using the training and validation data, respectively. Using the data, specific rate curve was prepared that explained the percentage of known landslide falling under the definite level of Landslide susceptibility Index. The classified values in the FR Model were than reclassified into 100 equal interval classes and rearranged in the descending order. Thus, for every 1 % interval classes, respective lower LSI limit values were recorded. Using the trapezoid method in Excel, the area under the curve (AUC) were then calculated [13], [21], [31].

The success rate diagram for the training data is shown in Figure 6. Similarly, the prediction rate diagram was also prepared using the similar process by using the testing data as shown in Figure 7.

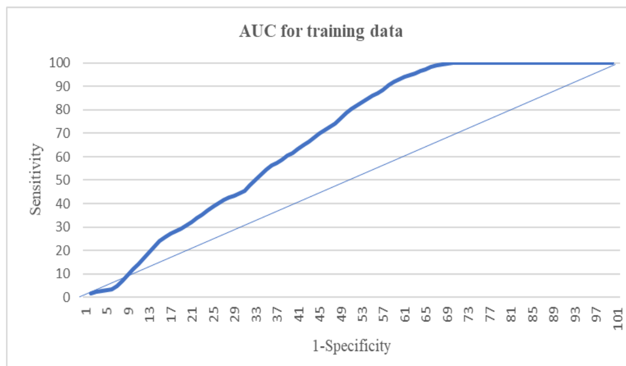

Figure 6: Success rate diagram using training data

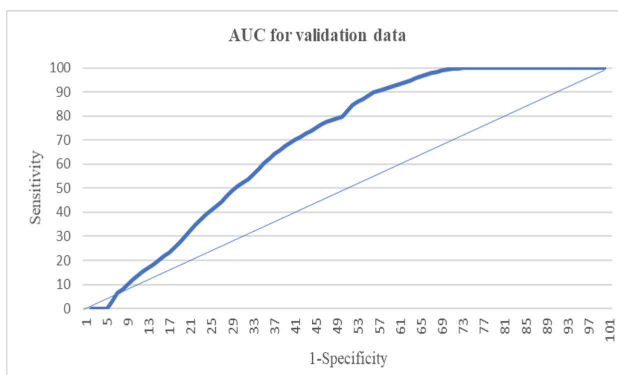

Figure 7: Prediction rate diagram using testing data

V. CONCLUSION

The results visualize the landslide susceptibility mapping of the Kaski district with help of twelve conditioning factors. It indicated that 32.09% of the area

e-ISSN: 2250-0758 | p-ISSN: 2394-6962
Volume-11, Issue-1 (February 2021)
https://doi.org/10.31033/ijemr.11.1.23

has very high and high landslide susceptibility while 15.93% of the area with moderate and 51.98% of the area with low and very low landslide susceptibility value. The modified FR analysis also gives the value of prediction rate for elevation (PR = 6.77), geology (PR= 6.45) and landcover (PR= 6.38) which are the most significant controlling factor for the Kaski district followed by the factors like rock type (PR = 5.57), precipitation (PR = 5.23), Aspect (PR = 4.89) and Slope (PR = 4.29) in our study. Similarly, the success and prediction rate of the modeled landslide susceptibility was found to be 67.68% and 68.87% respectively.

The developed landslide susceptibility map can be used for the different planning purposes and can also serve as a baseline information for the preparation of risk sensitive landuse planning.

REFERENCES

[1] P. Kayastha, F. Smedt, & M. Dhital. (2010). *GIS based landslide susceptibility assessment in Nepal Himalaya: A comparison of heuristic and statistical bivariate analysis*.

[2] F. Guzzetti, P. Reichenbach, M. Cardinali, M. Galli, & F. Ardizzone. (2005). Probabilistic landslide hazard assessment at the basin scale. *Geomorphology*, *72*(1–4), 272–299. DOI: 10.1016/j.geomorph.2005.06.002.

[3] A. K. Saha, R. P. Gupta, I. Sarkar, M. K. Arora, & E. Csaplovics. (2005). An approach for GIS-based statistical landslide susceptibility zonation-with a case study in the Himalayas. In: *Landslides, 2*(1), 61–69.
DOI: 10.1007/s10346-004-0039-8.

[4] F. Guzzetti, M. Galli, P. Reichenbach, F. Ardizzone, & M. Cardinali. (2006). Landslide hazard assessment in the Collazzone area, Umbria, Central Italy. *Nat. Hazards Earth Syst. Sci*., *6*(1), 115–131. DOI: 10.5194/nhess-6-115-2006.

[5] S. Sarkar & D. Kanungo. (2006). GIS based landslide susceptibility mapping—A case study in Indian Himalaya. *Proc. Interpraevent Int. …*, pp. 617–624.

[6] L. J. Wang, M. Guo, K. Sawada, J. Lin, & J. Zhang. (2015). Landslide susceptibility mapping in Mizunami City, Japan: A comparison between logistic regression, bivariate statistical analysis and multivariate adaptive regression spline models. *Catena*, *135*, 271–282.
DOI: 10.1016/j.catena.2015.08.007.

[7] F. Guzzetti, A. Carrara, M. Cardinali, & P. Reichenbach. (1999). Landslide hazard evaluation: A review of current techniques and their application in a multi-scale study, Central Italy. In: *Geomorphology, 31*(1–4), 181–216. DOI: 10.1016/S0169-555X(99)00078-1.

[8] S. D. Pardeshi, S. E. Autade, & S. S. Pardeshi. (2013). Landslide hazard assessment: Recent trends and techniques. *SpringerPlus*. DOI: 10.1186/2193-1801-2-523.

[9] E. A. Castellanos Abella & C. J. Van Westen. (2006). Qualitative landslide susceptibility assessment by multicriteria analysis: A case study from San Antonio del Sur, Guantánamo, Cuba. *Geomorphology*.
DOI: 10.1016/j.geomorph.2006.10.038.

[10] M. Ercanoglu, C. Gokceoglu, & T. W. J. Van Asch. (2004). Landslide susceptibility zoning north of Yenice (NW Turkey) by multivariate statistical techniques. *Nat. Hazards*, *32*(1), 1–23.
DOI: 10.1023/B:NHAZ.0000026786.85589.4a.

[11] H. J. Oh, S. Lee, & G. M. Soedradjat. (2010). Quantitative landslide susceptibility mapping at Pemalang area, Indonesia. *Environ. Earth Sci.*
DOI: 10.1007/s12665-009-0272-5.

[12] K. Solaimani, S. Z. Mousavi, & A. Kavian. (2013). Landslide susceptibility mapping based on frequency ratio and logistic regression models. *Arab. J. Geosci.*
DOI: 10.1007/s12517-012-0526-5.

[13] S. Lee & B. Pradhan. (2007). Landslide hazard mapping at Selangor, Malaysia using frequency ratio and logistic regression models. In: *Landslides*.
DOI: 10.1007/s10346-006-0047-y.

[14] T. H. Mezughi, J. M. Akhir, A. G. Rafek, & I. Abdullah. (2011). Landslide susceptibility assessment using frequency ratio model applied to an area along the E-W highway (Gerik-Jeli). *Am. J. Environ. Sci.*, *7*(1), 43–50.
DOI: 10.3844/ajessp.2011.43.50.

[15] S. Lee. (2005). Application of logistic regression model and its validation for landslide susceptibility mapping using GIS and remote sensing data. *Int. J. Remote Sens.* DOI: 10.1080/01431160412331331012.

[16] Desinventar. (2016). *Country profile of Nepal*. Available at: https://www.desinventar.net/.

[17] MoHA. (2020). *Nepal disaster risk reduction portal*. Available at: http://drrportal.gov.np/.

[18] V. Vakhshoori & M. Zare. (2016). Landslide susceptibility mapping by comparing weight of evidence, fuzzy logic, and frequency ratio methods. *Geomatics*, *Nat. Hazards Risk*. DOI: 10.1080/19475705.2016.1144655.

[19] A. D. Regmi *et al.* (2014). Application of frequency ratio, statistical index, and weights-of-evidence models and their comparison in landslide susceptibility mapping in Central Nepal Himalaya, *Arab. J. Geosci.*
DOI: 10.1007/s12517-012-0807-z.

[20] H. Shahabi, S. Khezri, B. Bin Ahmad, & M. Hashim. (2014). Landslide susceptibility mapping at central Zab basin, Iran: A comparison between analytical hierarchy process, frequency ratio and logistic regression models. *Catena, 115*, 55–70. DOI: 10.1016/j.catena.2013.11.014.

[21] C. J. F. Chung & A. G. Fabbri. (2003). Validation of spatial prediction models for landslide hazard mapping. *Nat. Hazards*.
DOI: 10.1023/B:NHAZ.0000007172.62651.2b.

[22] F. C. Dai, C. F. Lee, J. Li, & Z. W. Xu. (2001). Assessment of landslide susceptibility on the natural

terrain of Lantau Island, Hong Kong. *Environ. Geol.*, *40*(3), 381–391. DOI: 10.1007/s002540000163.
[23] S. Lee & J. A. Talib. (2005). Probabilistic landslide susceptibility and factor effect analysis. *Environ. Geol.* DOI: 10.1007/s00254-005-1228-z.
[24] A. Yalcin, S. Reis, A. C. Aydinoglu, & T. Yomralioglu. (2011). A GIS-based comparative study of frequency ratio, analytical hierarchy process, bivariate statistics and logistics regression methods for landslide susceptibility mapping in Trabzon, NE Turkey. *Catena*. DOI: 10.1016/j.catena.2011.01.014.
[25] S. Reis *et al.* (2012). Remote sensing and GIS-based landslide susceptibility mapping using frequency ratio and analytical hierarchy methods in Rize province (NE Turkey). *Environ. Earth Sci.* DOI: 10.1007/s12665-011-1432-y.
[26] S. Mondal & R. Maiti. (2013). Integrating the Analytical Hierarchy Process (AHP) and the frequency ratio (FR) model in landslide susceptibility mapping of Shiv-khola watershed, Darjeeling Himalaya. *Int. J. Disaster Risk Sci.* DOI: 10.1007/s13753-013-0021-y.
[27] S. Ghosh *et al.* (2012). Generating event-based landslide maps in a data-scarce Himalayan environment for estimating temporal and magnitude probabilities. *Eng. Geol.* DOI: 10.1016/j.enggeo.2011.03.016.
[28] D. M. Cruden & R. Fell. (1997). *Landslide risk assessment*. Available at: https://webapps.unitn.it/Biblioteca/it/Web/EngibankFile/3178275.pdf.
[29] S. Park, C. Choi, B. Kim, & J. Kim. (2013). Landslide susceptibility mapping using frequency ratio, analytic hierarchy process, logistic regression, and artificial neural network methods at the Inje area, Korea. *Environ. Earth Sci.* DOI: 10.1007/s12665-012-1842-5.
[30] R. Nagarajan, A. Roy, R. Vinod Kumar, A. Mukherjee, & M. V. Khire. (2000). Landslide hazard susceptibility mapping based on terrain and climatic factors for tropical monsoon regions. *Bull. Eng. Geol. Environ.* DOI: 10.1007/s100649900032.
[31] J. Choi, H. J. Oh, H. J. Lee, C. Lee, & S. Lee. (2012). Combining landslide susceptibility maps obtained from frequency ratio, logistic regression, and artificial neural network models using ASTER images and GIS. *Eng. Geol.* DOI: 10.1016/j.enggeo.2011.09.011.